RELATING DUST STORM MORPHOLOGY TO WAVE DYNAMICS.

J. M. Battalio, *Dept. of Earth and Planetary Sciences, Yale University, New Haven, CT (joseph.battalio@yale.edu).*

Introduction

Our understanding of Mars's weather and dust storms has accelerated over the past decades. Many large dust storms originate in the northern hemisphere and are caused by traveling baroclinic waves; however, the relationships between specific dynamical structures within these waves and the morphology of visible dust features remains poorly constrained. With the development of observation-based reanalysis datasets, the evolution of dust activity and their incipient wave structures can be better determined. In combination, these datasets can verify the positions of air masses, cyclones, and fronts in relation to visible structures in dust activity, which are needed to validate weather models, and will further improve our understanding of the Martian dust cycle.

Mars's Major Dust Storms

Most dust storm activity is confined along the edge of the ice caps, but organized events flush equatorward [1–3]. Cross-equatorial storms traverse through three northern topographic channels: Acidalia, Utopia, and Arcadia Planitiae in a ratio of 4:2:1 [2]. Northern flushing events with a large southern hemispheric component that occur during L_s = 180–250° are deemed "A" events, and similar events occurring during L_s = 300–360° are "C" events [4]. In between, a break in northern hemisphere activity is called the solstitial pause [5;6]; at this time, a "B" storm occurs along the southern hemisphere cap edge.

Dust events come in multiple morphologies and textures [7;8]. This variety complicates the identification of fronts, cyclones, or other hallmarks of atmospheric waves from orbital mapping alone. The coarse resolution of most global models and an inability to connect visible features from orbit to the wave structures prevents models from fully representing this variety of morphologies [9]. Therefore, to interpret these structures, we combine datasets relate dust to dynamics.

Transient Waves on Mars

Organized dust event initiation and growth is strongly linked to traveling waves [10;11]. This link is casually reinforced by the observation that after major dust sequences, there is a period of reduced dust storms coinciding with weakened transient eddies. Eddies are weakened by the additional dust after flushing stabilizes the atmosphere [1;12;13]. Many waves that cause dust events are generally baroclinic, meaning they initiate due to equator-to-pole temperature differences, and are similar in size to midlatitude waves on Earth [13–15]. From orbital observations, Martian baroclinic waves have periods of 2–10 sols, zonal wave numbers of 1–3 [16–18], and are larger amplitude in the northern hemisphere [15;19].

However, free-running model simulations disagree on the dominant wave periodicity and zonal wavenumber [14;20]. Even reanalyses constrained by observations can exhibit differences in wave properties for the same time [18;19] (Fig. 1). Most large-scale dust storms on Mars appear to be generated by cyclones embedded within traveling wave structures. These waves are induced by the same baroclinic instability that creates terrestrial extra-tropical cyclones. Thus, an independent dust storm dataset will constrain models and capture the timing of opacity changes within cyclone structures (i.e., direction of winds, pressure, and temperature changes).

The Mars Dust Activity Database (MDAD, v1.0)

Near-continuous imaging permits documentation of the occurrence and morphology of dust activity. These data are currently available in the Mars Dust Activity Database (MDAD) [2], which is created from Mars Daily Global Maps (MDGM). The MDAD catalogs dust storm activity with well-defined boundaries between L_s = 150°, MY 24 and L_s = 171°, MY 32. The MDAD contains the time, centroid, area, maximum and minimum latitudes, and IDs for 14,974 storm instances. A confidence level is subjectively assigned to each storm (25, 50, 75, or 100) to describe the accuracy of the storm boundaries. A unique dust storm member ID is given to each dust storm; thus, a dust storm member consists of a single dust storm occurring on one or more consecutive sols. Organized dust events are identified as dust storm "sequences," which are collections of one or more dust storm members that follow a similar trajectory [1;2;22]. Sequences have a duration of $\geq$3 sols.

Martian Reanalysis Datasets

A recent leap in capabilities of weather diagnosis comes from the development of multiple Martian reanalysis datasets. Reanalyses combine observations and global circulation models to produce regular time-series of the atmospheric state. They are therefore superior for analyzing the dynamics of Mars versus raw vertical profiles or observations, as they are self-consistent, validated against observations, and provide wind data.

Multiple reanalyses exist for Mars: The Open access to Mars Assimilated Remote Soundings (OpenMARS, v1.0 [21]) covers L_s = 98°, MY 24 to L_s = 351°, MY 32. OpenMARS has a 5° × 5° horizontal resolution with 25 vertical levels every two hours. The Ensemble Mars Atmospheric Reanalysis System (EMARS, v1.0 [23]) spans L_s = 103°, MY 24 to L_s = 105°, MY 33. EMARS is an ensemble dataset, meaning that the model is run multiple times with slightly different parameters to capture atmospheric uncertainty. EMARS has a 6° longitude × 5° latitude horizontal resolution with 28 levels.

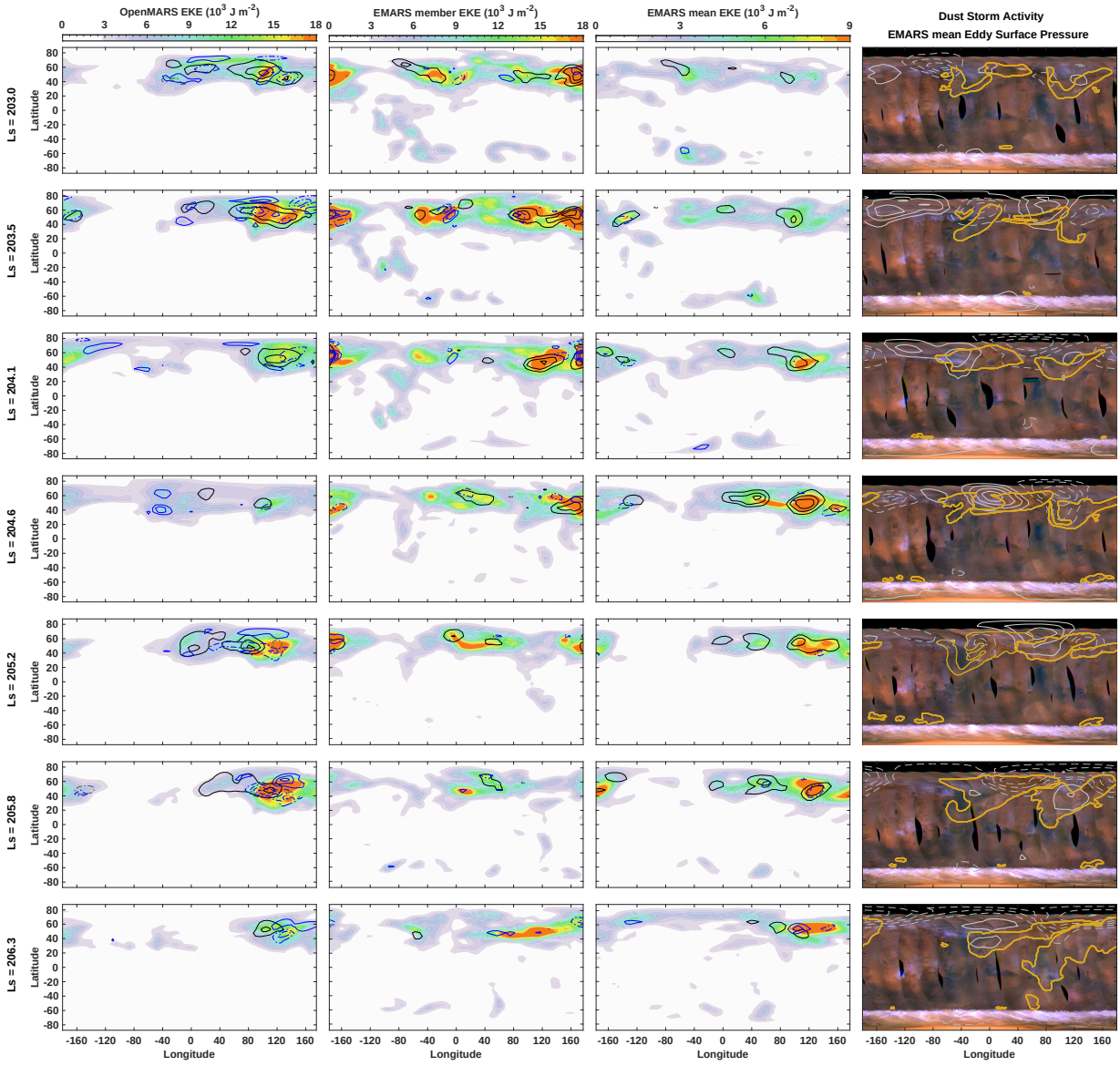

Figure 1: Progression of eddies from MY 31 in OpenMARS (first column), EMARS member (second column), and EMARS ensemble mean (third column). In columns 1–3, eddy kinetic energy is shaded, and baroclinic energy conversion (red contours) and barotropic energy conversion (blue contours) are contoured every 0.2 W m^{-2} for OpenMARS and EMARS ensemble mean and 0.4 W m^{-2} for EMARS member, with negative values dashed. MDGMs are shown in column 4, with dust activity from the MDAD[2] outlined in gold. Eddy surface pressure from the EMARS ensemble is contoured every 8 Pa, with negative values dashed. Each row is averaged for ∼1 sol starting with the L_s listed at left, corresponding to the MDGMs. Adapted from Battalio (2022)[5].

Comparison of dust storms to wave dynamics

From each reanalysis, the appropriate wave periods for dust-storm incipient baroclinic waves are filtered from the surface pressure, wind, and temperature fields. The wave energy (eddy kinetic energy, EKE), the main growth mechanism of baroclinic waves (baroclinic energy conversion, BCEC), and the main decay process of the waves (barotropic energy conversion, BTEC) are derived[5]. This analysis is only possible with a reanalysis dataset since free-running model simulations lack direct connection to specific, observed dust events.

With the filtered data extracted, the reanalysis fields are juxtaposed with MDGMs showing the dust activity. Figure 1 shows one of the major contributing wave groups to the "C" dust event in MY 31. Initially, EKE and BCEC at L_s=203.0° are found in Acidalia and Utopia, as dust storms are ongoing. Over the next two sols (L_s=203.5°and L_s=204.1°), EKE and BCEC in Acidalia move east through Utopia, where BTEC becomes negative. As this occurs, a new dust event passes into Utopia from Acidalia. From L_s=204.6°, the new region of EKE baroclinically develops in Acidalia in the following two days (L_s=205.2°and L_s=205.8°), with BTEC decay occurring on the last sol (L_s=206.3°). Between L_s=204.6° and L_s=206.3°, a new dust event develops in

Acidalia and flushes south with this eddy. Individual waves travel around the latitude circle as a repeating progression of eddy surface pressure anomalies (Fig. 1, column four, contours), but both EMARS and OpenMARS pinpoint Utopia as a region of continuous EKE throughout the period. The activity in Utopia is not a stationary wave, but instead eddy amplification occurs as waves pass through storm regions.

The novel approach to apply reanalyses illuminates the dynamics that cause dust storm behavior, captured in Fig. 2. The synoptic setup from OpenMARS (left) and EMARS member (right) are overlain on the twinned, flushing dust event from Fig. 1. Now, we analyze the dynamical structures behind the dust event. Each row of Fig. 2 repeats the MDGM and MDAD outlines from Fig. 1 (right column). The frontal structure, high and low pressure, and eddy surface temperatures show that the eddy features from Fig. 1 emerge from two extratropical, low-pressure cyclones. The eddy wind field (vectors) demonstrates the undulating nature of the waves along 60°N, with equatorially directed motions where dust is transported south (between 75° and 130°E in Utopia and again between -50° and 10°E in Acidalia). Further, the associated eddy surface pressures (white contours) indicate that high pressure upstream of the edge of the dust extends further south than the low pressure regions downstream of the dust storms.

While the above case exhibits good agreement between reanalyses at most times, there are instances of disagreement. For example, the EMARS member consistently has an amplified eddy pressure regime in the western hemisphere (over Arcadia and Tharsis), while such features are absent with OpenMARS (Fig. 2). Due to the occasional poor match between reanalyses for some sols as a result of poorly constrained low-level temperatures[5], diagnostic analysis should be used cautiously on only one reanalysis at a time; however, there is considerably more agreement between reanalyses and within the EMARS ensemble versus free-running simulations[23]. To completely rectify any disagreement between datasets, additional observational platforms in the form of surface observation stations networks, areostationary satellite constellations, or additional polar-orbiting satellites will be required to improve the quality of reanalyses. At least, a priority should be redundancy in the case of loss of MRO. Regardless, that separate reanalyses agree on the broad placement of wave structures in the context of visible frontal dust systems as seen in the independently collected Mars Dust Activity Database[2] increases the overall confidence in the accuracy of each dataset.

Summary

With the advent of reanalysis datasets, the dynamics of individual traveling waves can be connected to the occurrence of dust activity, generating climatologies of synoptic cyclones. These datasets and orbital observations demonstrate a variety of dust storm morphologies. Despite rapid improvements, atmospheric models struggle to simulate the menagerie of dust storm structures, particularly the development of regional dust storms. By mapping the structure of dust transported by an atmospheric wave and diagnosing the timing, amplitude, and phase of waves required to achieve flushing, we can better determine how dust is transported by cyclones.

Case studies of large dust storms in the Martian northern hemisphere are selected from the Mars Dust Activity Database[2] and compared to wave activity as diagnosed in reanalysis datasets. The wave winds and temperature structures are compared to the morphology of the dust storms, and the sources of eddy energy are evaluated. Frontal structures exhibited by the dust storms compare well to near-surface wave structures, including wind shifts and surface cyclones/anti-cyclones. Dust event evolution shares similarities to the terrestrial paradigm of extra-tropical cyclogenesis, maturity, and decay. These results point to the development of cyclone models for Mars, which may enable better inter-seasonal and inter-annual comparisons.

Future work will analyze the energetics of Mars's transient waves by zonal wavenumber, applying the analysis of Battalio & Wang (2020)[1] to a full energetics perspective to assess inter-annual variability. An open question is the precise nature of the solstitial pause, with regard to reductions in baroclinic activity being an intrinsic property of storm tracks. Quantification of the agreement between reanalysis datasets may provide the community an objective way to evaluate when the reanalyses are most likely to represent the true atmospheric state. Finally, a more comprehensive analysis of dust activity from the Mars Dust Activity Database[2] and their incipient transient waves may provide better diagnostic evidence of dust and wave evolution.

Acknowledgments

The Mars Dust Activity Database (v1) is available at doi:10.7910/DVN/F8R2JX. MDGMs (v2) are available at doi:10.7910/DVN/U3766S. Reanalyses are available at: MACDA (doi:10.5285/78114093-E2BD-4601-8AE5-3551E62AEF2B); EMARS (doi:10.18113/ D3W375); OpenMARS (doi:10.21954/ou.rd.c.4278950).

References: [1] Battalio et al. 2020, Icar., 338, 113507. [2] Battalio et al. 2021, Icar., 354, 114059. [3] Wang et al. 2015, Icar., 251, 112. [4] Kass et al. 2016, GRL, 43. [5] Battalio, J. M. 2022, JAS, 79, 361. [6] Lewis et al. 2016, Icar., 264, 456. [7] Kok et al. 2012, Rep. on Prog. in Phys., 75. [8] Guzewich et al. 2017, Icar., 289, 199. [9] Hollingsworth et al. 2010, GRL, 37, 3. [10] Wang et al. 2003, GRL, 30, 1488. [11] Mooring et al. 2015, JGR: P, 120, 1. [12] Hinson et al. 2021, Icar. [13] Battalio et al. 2016, Icar., 276, 1. [14] Wang et al. 2013, Icar., 223, 654. [15] Battalio et al. 2018, Icar., 309, 220. [16] Banfield et al. 2003, Icar., 161, 319. [17] Hinson et al. 2010, Icar., 206, 290. [18] Greybush et al. 2019, Icar., 317, 158. [19] Battalio et al. 2021, Nat. Astr., 5, 1139. [20] Greybush et al. 2013, QJRMS, 139, 639. [21] Holmes et al. 2020, PSS, 188, 104962. [22] Battalio et al. 2019, Icar., 321, 367. [23] Greybush et al. 2019, Geosci. Data J., 6, 137.

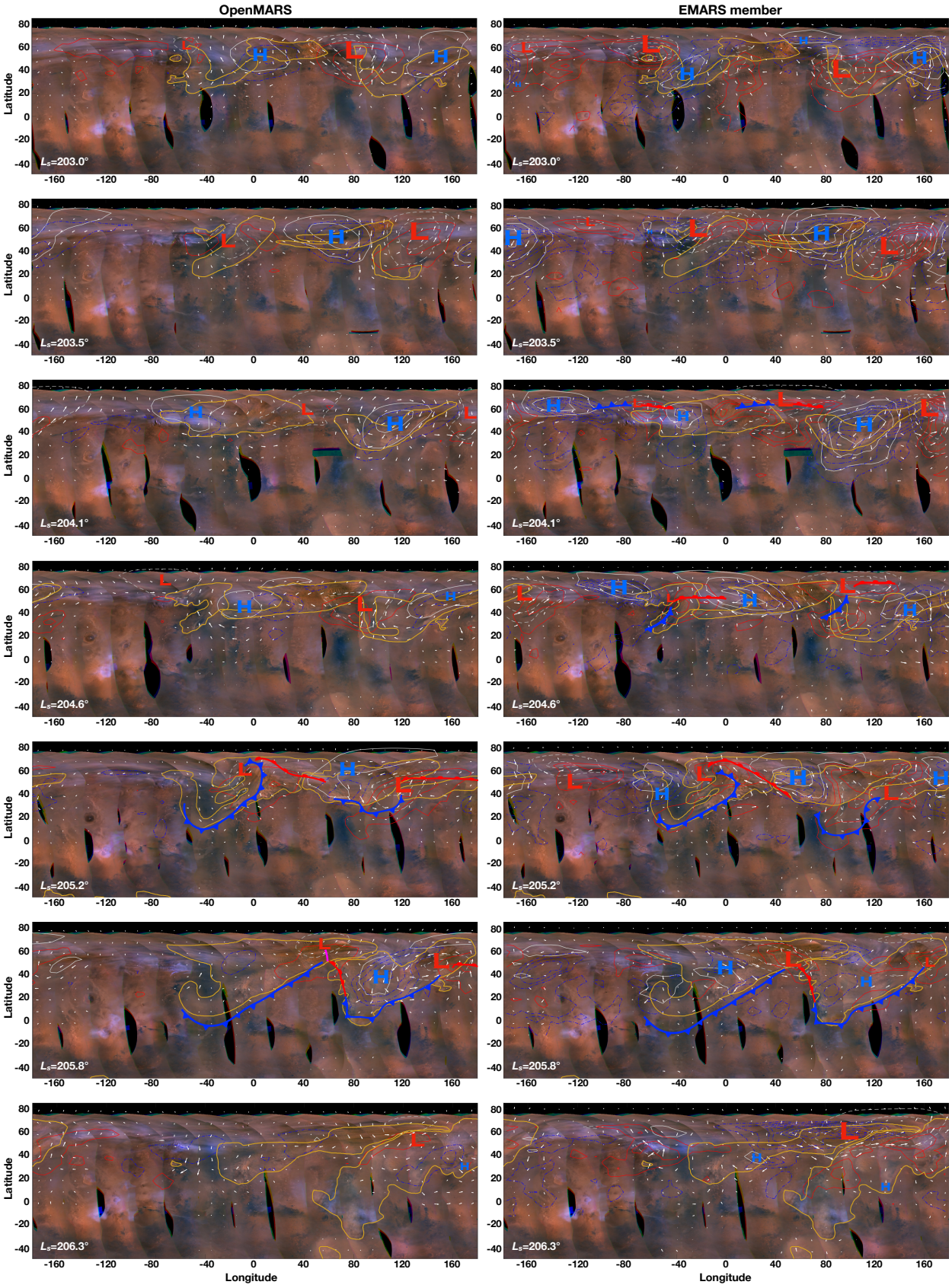

Figure 2: Seven sols from Mars year 31 Mars Daily Global Maps and Mars Dust Activity Database indicated dust activity (gold contours)[2]. Eddy winds (vectors), eddy surface pressure pressure (white contours every 0.4 Pa with negative values dashed and extrema indicated with blue "H" and red "L"), eddy surface temperature (red/blue contours every 1 K with solid red positive and dashed blue negative) provided by either OpenMARS[21] or EMARS ensemble member[18] renalyses with surface fronts drawn.